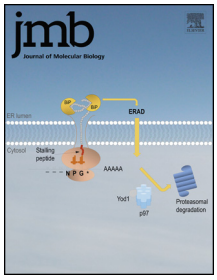

Contacts in Death: The Role of the ER–Mitochondria Axis in Acetic Acid-Induced Apoptosis in Yeast

Vítor M. Martins [1], Tânia R. Fernandes [1], Diana Lopes [2,3], Catarina B. Afonso [1], Maria R.M. Domingues [2,3], Manuela Côrte-Real [1] and Maria J. Sousa [1]

1 - Centre of Molecular and Environmental Biology, *Department of Biology, University of Minho, Campus de Gualtar, 4710-057 Braga, Portugal*
2 - Mass Spectrometry Centre, *Department of Chemistry & QOPNA, University of Aveiro, Campus Universitário de Santiago, 3810-193 Aveiro, Portugal*
3 - Department of Chemistry & CESAM & ECOMARE, *University of Aveiro, Campus Universitário de Santiago, 3810-193 Aveiro, Portugal*

Correspondence to Vítor M. Martins and Maria J. Sousa: *vitor.rmmartins@gmail.com, mjsousa@bio.uminho.pt*
https://doi.org/10.1016/j.jmb.2018.11.002
Edited by M Yaniv

Abstract

Endoplasmic reticulum–mitochondria contact sites have been a subject of increasing scientific interest since the discovery that these structures are disrupted in several pathologies. Due to the emerging data that correlate endoplasmic reticulum–mitochondria contact sites function with known events of the apoptotic program, we aimed to dissect this interplay using our well-established model of acetic acid-induced apoptosis in *Saccharomyces cerevisiae*. Until recently, the only known tethering complex between ER and mitochondria in this organism was the ER–mitochondria encounter structure (ERMES). Following our results from a screening designed to identify genes whose deletion rendered cells with an altered sensitivity to acetic acid, we hypothesized that the ERMES complex could be involved in cell death mediated by this stressor. Herein we demonstrate that single ablation of the ERMES components Mdm10p, Mdm12p and Mdm34p increases the resistance of *S. cerevisiae* to acetic acid-induced apoptosis, which is associated with a prominent delay in the appearance of several apoptotic markers. Moreover, abrogation of Mdm10p or Mdm34p abolished cytochrome *c* release from mitochondria. Since these two proteins are embedded in the mitochondrial outer membrane, we propose that the ERMES complex plays a part in cytochrome *c* release, a key event of the apoptotic cascade. In all, these findings will aid in targeted therapies for diseases where apoptosis is disrupted, as well as assist in the development of acetic acid-resistant strains for industrial processes.

Introduction

Mitochondrial outer membrane permeabilization (MOMP) and release of pro-apoptotic factors such as cytochrome *c* from mitochondria to the cytosol have been considered "the point of no return" of apoptosis [1]. Although extensive research has been performed to uncover the molecular machinery that underlies MOMP formation, there is still a lack of consensus on this matter. The initial model postulated that this phenomenon was regulated by a supramolecular complex known as the mitochondrial permeability transition pore (mPTP). This channel crosses both mitochondrial membranes and allows the passage of solutes up to 1.5 kDa, resulting in an increased osmotic pressure that leads to mitochondrial swelling and eventual mitochondrial outer membrane (MOM) rupture [2,3]. Numerous mitochondrial proteins have been implicated in the structure and regulation of mPTP, such as the voltage-dependent anion channel (VDAC), the adenine nucleotide translocator (ANT), cyclophilin D, the peripheral benzodiazepine receptor, the inorganic phosphate carrier and the F_O–F_1 ATP synthase [4]. However, throughout the years, evidence has arisen to dispute the involvement of each of these components in apoptosis, and mPTP formation is now believed to be more representative in necrotic cell death [5–13]. In the midst of these discoveries, it was shown that cytochrome *c* release can also occur without loss of mitochondrial integrity, suggesting that an alternative mechanism of permeabilization exists such as a MOM pore [14]. Indeed, it is now widely

accepted that pro-apoptotic proteins from the Bcl-2 family of proteins, such as Bax and Bak, are activated in response to apoptotic stimuli and are capable of forming a pore in the MOM, known as mitochondrial apoptosis-induced channel, to release pro-apoptotic proteins. Nonetheless, taking into account that this channel has a relatively small size, it still does not explain how certain apoptogenic molecules cross the MOM [15,16]. As such, a consensual and decisive model describing the molecular regulation of MOMP is still missing.

In the scope of cell death, our laboratory has previously described that the yeast *Saccharomyces cerevisiae* commits to an active cell death process in response to acetic acid with morphological and functional alterations that are typical of mammalian apoptosis [17,18]. For years it was thought that yeast lacked obvious orthologues of mammalian pro-apoptotic Bcl-2 proteins. However, it was recently found that similarly to these, the yeast protein Ybh3p contains a functional BH3 domain that is able to interact with Bcl-xL and activate the mitochondrial pathway upon apoptotic stimuli [19]. Even so, the question remains as to which are the main regulators of MOMP in this organism. Several yeast genes have been linked to acetic acid-induced apoptosis, with many of their orthologues also being described as regulators of mammalian apoptosis [18,20–28]. Specifically regarding MOMP formation, we have previously described the involvement of Aac1/2/3 (yeast ANT) and Por1p (yeast VDAC) in acetic acid-induced apoptosis. Absence of Aac1/2/3 inhibited cytochrome *c* release after acetic acid challenge while *POR1* deletion sensitized cells exposed to this stressor [25]. A later study revealed that the sensitivity to acetic acid displayed by *por1*Δ mutants is abrogated by further deletion of the Aac1/2/3 proteins, suggesting that Por1p may function as a negative regulator of cell death by inhibiting the pro-death role of Aac1/2/3 [29]. Considering that these are membrane proteins with described roles in mammalian MOMP, it is likely that the altered sensitivity of these deletion mutants is due to an active role in MOMP formation. It was also shown that acetate is able to induce a mitochondria-dependent apoptotic cell death in colorectal carcinoma cell lines [30], which we have since explored to assess the mechanistic effect of acetate and its possible use as a prophylactic agent [31–33]. Combined with the fact that enhanced acetic acid-resistant yeast strains are required for industrial processes, such as lignocellulosic fermentation, the elucidation of the molecular mechanisms underlying acetate/acetic acid-induced apoptosis in colorectal carcinoma/yeast cells will bring about both biomedical and biotechnological interest.

In order to identify genes whose deletion induced an altered sensitivity to acetic acid-induced apoptosis, we have recently performed a genetic screening on the EUROSCARF haploid mutant collection [34]. In this screening, we found that strains lacking proteins involved in endoplasmic reticulum–mitochondria tethering displayed different sensitivity to acetic acid challenge.

Endoplasmic reticulum–mitochondria contact sites (ER-MCS), found from yeast to mammals, are interface structures where membranes of the two organelles are maintained in close apposition by tethering protein complexes. These contact sites have been the subject of increasing interest as data point to a prominent role in the communication between the two organelles, including the transport of metabolites and transmission of cellular cues that can regulate ER and mitochondrial biology [35–37]. In metazoans, ER-MCS are composed of several protein complexes involving mitofusins 1 and 2 (Mfn1/2), the inositol 1,4,5-trisphosphate receptor (IP_3R), the phosphofurin acidic cluster sorting protein 2 (PACS-2), VDAC and several others [38,39]. Conversely, until recently the only known tethering complex between the ER and mitochondria in *S. cerevisiae* was the ER–mitochondria encounter structure (ERMES) [40]. ERMES, which is localized in discrete foci between the ER membrane and the MOM, is a heterotetrameric complex composed of a nucleus of four proteins: the ER-anchored protein Mmm1p, cytosolic Mdm12p and two MOM proteins Mdm10p and Mdm34p [37]. This complex is thought to be regulated by a calcium-binding Miro-GTPase that controls the number and size of ERMES, Gem1p [41,42], although this association has been disputed [43]. In addition to being implicated in lipid and calcium exchange [44], ERMES has been also correlated with anchoring mitochondrial DNA (mtDNA) nucleoids and mtDNA replication [45–47], mitochondrial inheritance [48], mitochondrial protein import and assembly of β-barrel proteins in the MOM [49], mitophagy [50], iron homeostasis [51] and in the association of mitochondria with the actin cytoskeleton [52]. Importantly, a Mmm1p orthologue was recently identified and found to regulate calcium dynamics in mammalian neurons, emphasizing that yeast ER-MCS are at least partially conserved in evolution [53].

Recent studies on mammalian cells have implicated ER-MCS in the mediation of apoptotic signals and subsequent induction of mitochondrial alterations leading to cell death, namely MOMP and cytochrome *c* release, two key events in the apoptotic process [54]. It was demonstrated that at these contact sites, the MOM is enriched in VDAC, which is a putative component of the mPTP [37,55]. Considering the role of excessive mitochondrial calcium intake in apoptosis [56] and that this phenomenon takes place in sites where ER and mitochondria are in close proximity [57], MOMP regulation by mitochondrial calcium overload very likely involves ER–mitochondria tethering complexes. Moreover, the ERMES complex has also been shown to be the site of Dnm1p recruitment and ensuing mitochondrial fragmentation [47], a process that occurs early in apoptosis [58]. Thus, in this work, we aimed to

unravel the role of the ERMES complex in acetic acid-induced apoptosis, namely, its potential involvement in the intricate molecular machinery that promotes MOMP.

Results

The ERMES complex components Mdm10p, Mdm12p and Mdm34p are required for acetic acid-induced apoptosis

To assess the overall susceptibility of yeast strains lacking ERMES complex components (*mdm10*Δ, *mdm12*Δ and *mdm34*Δ) toward acetic acid stress, we first evaluated clonogenic survival of wild-type and mutant strains after exposure to 100 mM acetic acid. All mutant strains revealed a significant increase in clonogenic ability in comparison to the wild-type strain (Fig. 1a). Impressively, *mdm34*Δ cells displayed a tremendous resistance to this stressor, with survival percentage of 84.2% ± 11.2% after 200 min of treatment *versus* 0.1% ± 0.2% for the wild-type strain. To infer if this particular acetic acid concentration could be triggering a necrotic cell death process in the wild-type strain, cells were stained with the DNA-intercalating dye propidium iodide (PI) and analyzed by flow cytometry (Fig. 1b). This dye can only enter the cell if the plasma membrane is disrupted, an event that occurs early in necrosis but later in the yeast apoptotic process. After 120 min of treatment, only 10.4% ± 0.3% of wild-type cells exhibited plasma membrane disruption, although survival had decreased 97.6% ± 3.3%, suggesting that cell death under these conditions was non-necrotic. Moreover, all mutant strains revealed a significant delay in the loss of plasma membrane integrity, corroborating an executor role of ERMES components in acetic acid-induced apoptosis.

ERMES deficiency perturbs mitochondrial function and delays the emergence of typical apoptotic events after acetic acid challenge

We have previously reported that *S. cerevisiae* W303-1A mitochondrial membrane suffers a quick hyperpolarization followed by depolarization after acetic acid treatment [18,26]. As such, we next assessed if these mutant strains presented alterations in mitochondrial transmembrane potential ($\Delta\Psi_m$) after exposure to this stressor. For that purpose, wild-type and ERMES-deficient cells along treatment were stained with the potential-sensitive probe $DiOC_6(3)$ and analyzed by flow cytometry. As we were only interested in evaluating these alterations at the beginning of the death process, samples were also co-stained with PI to select only the PI-negative sub-population for analysis. Moreover, since mitochondrial mass varies with cell size, $DiOC_6(3)$ signal was normalized over cell volume [59]. In agreement with our previous results using this probe [26], wild-type mitochondria suffered a quick hyperpolarization after 60 min of treatment and reached a plateau throughout the assay, which eventually slightly reduced at 200 min (Fig. 2). Not surprisingly, the $\Delta\Psi_m$ of the mutant strains remained practically unchanged for the first hour of treatment. Thereafter, the $\Delta\Psi_m$ of *mdm10*Δ and *mdm12*Δ seemed to follow in the same pattern as the wild-type strain, while *mdm34*Δ mitochondria appeared to only slightly hyperpolarize. Thus, it appears that alteration of mitochondrial membrane potential and loss of cell survival are synced events since the latter only occurs when mitochondria start to

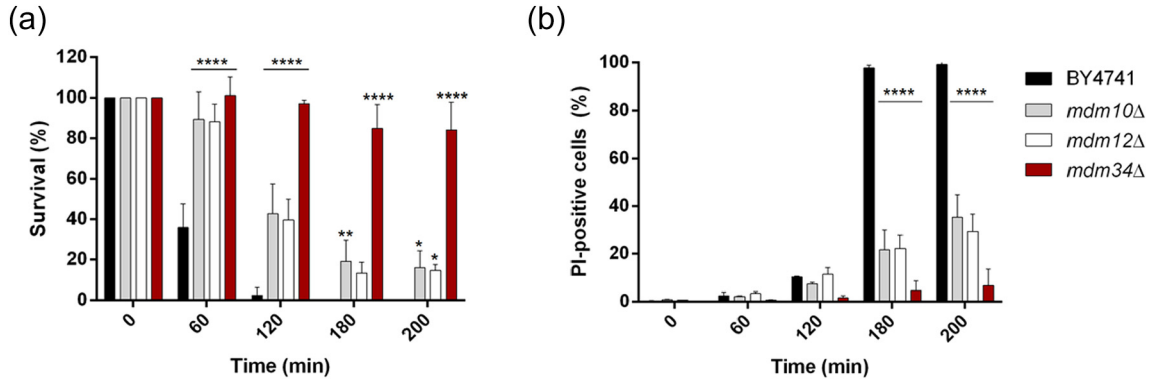

Fig. 1. Absence of ERMES complex components enhances cell survival and delays loss of plasma membrane integrity after acetic acid treatment. Exponential phase cells were treated for 200 min with 100 mM acetic acid. (a) Clonogenic survival was assessed by CFU counts on YEPDA plates, where time zero was considered 100% of cell viability. (b) At each time point, plasma membrane integrity was evaluated by staining with 1 μg/mL PI for 10 min. The results are expressed as mean ± SD of four (a) and two (b) independent experiments (two-way ANOVA, Dunnett's *post hoc* test: $^*p < 0.05$, $^{**}p < 0.01$, $^{****}p < 0.0001$).

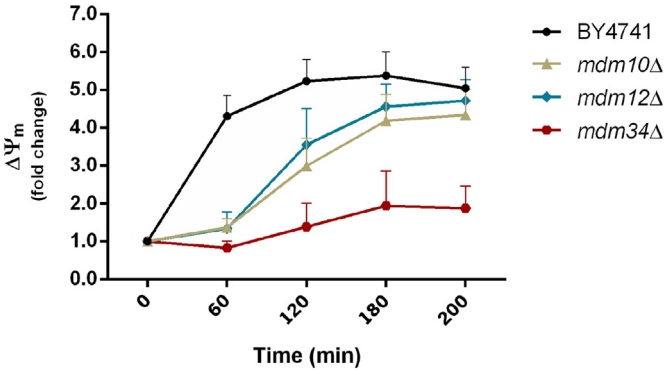

Fig. 2. Alteration of mitochondrial transmembrane potential is delayed in yeast lacking ERMES components upon acetic acid challenge. Relative $DiOC_6(3)$ fluorescence of exponential phase cells exposed to 100 mM acetic acid for 200 min. At each time point, cells were harvested and co-stained with 1 nm $DiOC_6(3)$ and 1 μg/mL PI before flow cytometry analysis. Mean fluorescence intensity of $PI^-/DiOC_6(3)^+$ cells was normalized to cell size. Results represent mean ± SD of three independent experiments.

become hyperpolarized (60 min for the wild-type and 120 min for *mdm10*Δ and *mdm12*Δ). This correlation is further corroborated by *mdm34*Δ in which significant changes are not observed, both in clonogenicity and in mitochondrial membrane potential during acetic acid treatment.

Yeast cells lacking ERMES components are reportedly defective in mitochondrial morphology, often displaying a giant spherical structure [48,60,61]. To evaluate if our mutant strains also displayed this phenotype, both wild-type and mutant strains were transformed with a plasmid carrying a mitochondrial

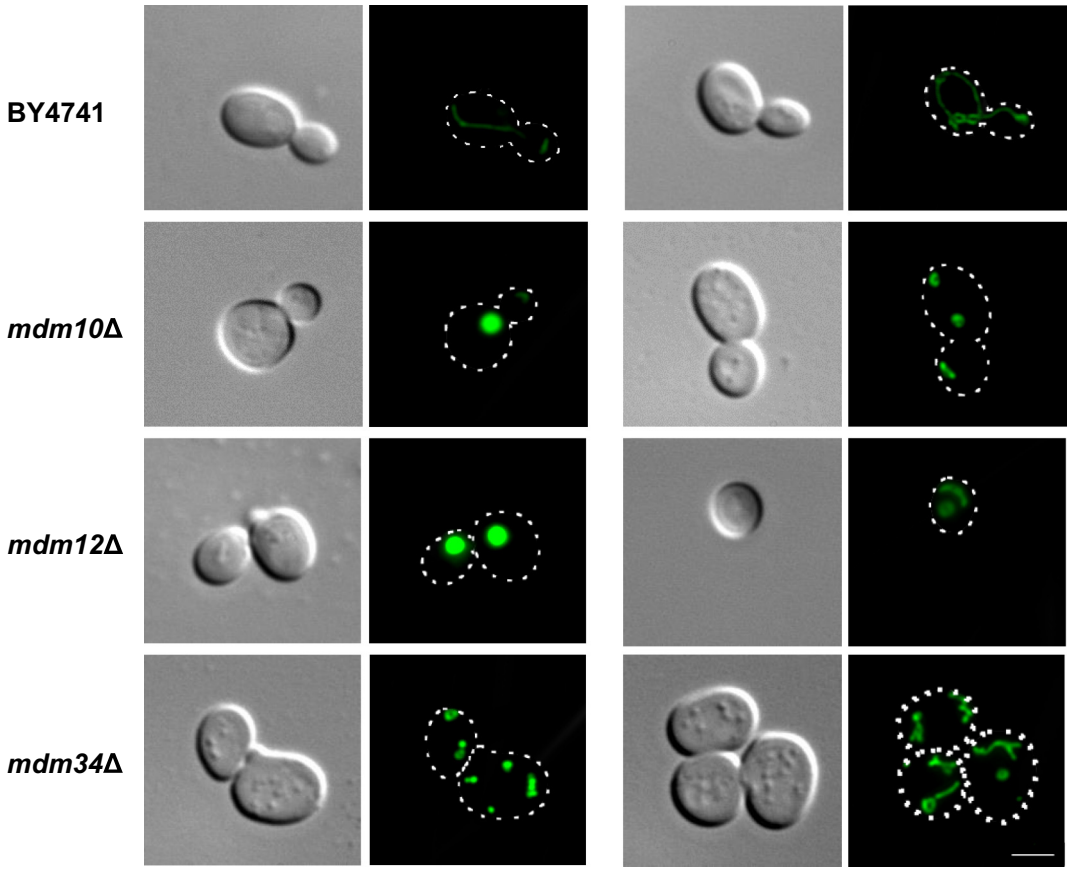

Fig. 3. Photomicrographs of yeast cells lacking ERMES complex components reveal impaired mitochondrial morphology. Wild-type and ERMES-deficient cells were transformed with a plasmid encoding a mitochondrial matrix-targeted green fluorescent protein (pYX242-mtGFP). Mitochondrial morphology of exponential phase yeast cells carrying the plasmid was assessed by fluorescence microscopy. Two examples per strain are shown to depict the different phenotypes encountered. The bar represents 5 μm.

matrix-targeted green fluorescent protein (pYX242-mtGFP) and mitochondrial morphotypes were visualized by fluorescence microscopy (Fig. 3). As expected, wild-type cells exhibited mitochondrial networks in the form of long linear threads. On the other hand, a very little percentage of ERMES-deficient cells revealed a similar phenotype. Both *mdm10*Δ and *mdm12*Δ strains predominantly revealed large and round mitochondria, with few cells exhibiting small punctae and/or short tubules. However, this morphotype was not found for the *mdm34*Δ strain, which only displayed either punctate or short tubular mitochondria in agreement with a previous study [62].

We next assessed if the mutant strains presented differences in mitochondrial degradation upon acetic acid treatment in comparison to the wild-type strain. For this purpose, we monitored the percentage increase of cells exhibiting lower GFP fluorescence levels than untreated cells as a marker of mitochondrial breakdown. The results revealed a quick increase in mitochondrial degradation for the wild-type strain that was not evidenced for the mutant strains (Fig. 4). After 200 min of treatment, wild-type cells exhibited only 25.9% ± 12.0% of cells with GFP fluorescence intensity similar to untreated cells while ERMES-deleted strains still exhibited a minimum of 72.5% ± 2.5%. It has been also reported that acetic acid-induced apoptosis of *S. cerevisiae* is accompanied by ROS accumulation, specifically superoxide anion [18,63]. To further characterize the response of ERMES-deleted strains to acetic acid, we assessed the accumulation of this ion by dihydroethidium (DHE) staining followed by flow cytometry analysis. The results showed an earlier increase in superoxide anion levels in the wild-type strain in comparison to the mutant strains (Fig. 5). While wild-type cells exhibited

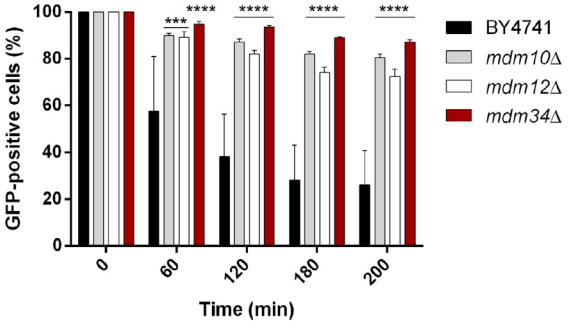

Fig. 4. Mitochondrial degradation upon acetic acid challenge is significantly delayed in ERMES-deficient cells. Wild-type and mutant strains carrying the pYX242-mtGFP plasmid were grown to exponential phase and treated with 100 mM acetic acid. The percentage of cells exhibiting green fluorescent mitochondria at time 0 was considered 100%, and values obtained for each time point were normalized to those of time 0. Data represent mean ± SD of three independent experiments (two-way ANOVA, Dunnett's *post hoc* test: ***$p < 0.001$, ****$p < 0.0001$).

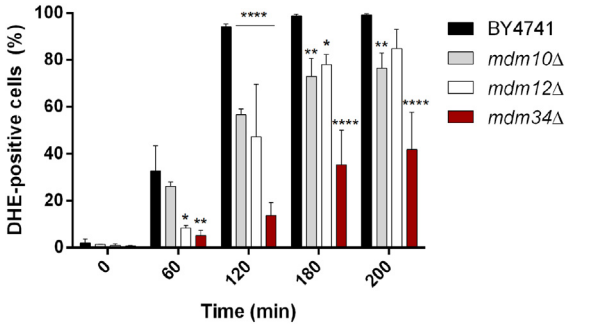

Fig. 5. Superoxide anion accumulation is significantly delayed in ERMES-deficient cells after acetic acid treatment. Exponential phase cells were treated with 100 mM acetic acid. At each time point, cells were stained with 2 μg/mL DHE for 20 min to evaluate accumulation of superoxide anion by flow cytometry. Results are reported as mean ± SD of three independent experiments (two-way ANOVA, Dunnett's *post hoc* test: *$p < 0.05$, **$p < 0.01$, ****$p < 0.0001$).

94.1% ± 1.0% of DHE-positive cells after 120 min, all mutant strains displayed a considerably lower percentage of cells with superoxide anion accumulation. Not surprisingly, at that particular time point, *mdm34*Δ revealed a tremendous delay in the accumulation of this ion, approximately seven times lower than the wild-type.

Absence of ERMES complex components reduces the yeast chronological life span and affects both respiratory ability and growth at restrictive temperature

Several reports have described that ERMES-deficient strains exhibit impaired respiratory ability [40,64,65]. Considering that respiratory-null (ρ^0) strains have increased resistance to acetic acid [18], it was necessary to discard the resistance of these mutants as being due to an inability to respire. Thus, wild-type and mutant strains were grown on solid glycerol plates, a non-fermentable carbon source where respiratory-deficient cells cannot grow. The results showed that *mdm10*Δ and *mdm12*Δ appear to have deficiencies in their respiratory capacities, while *mdm34*Δ exhibits a wild-type-like phenotype (Fig. 6a, right panel). The mutants also grew in liquid glycerol media, albeit more slowly than the wild-type. The characterization of mitochondrial morphotypes by fluorescence microscopy (Fig. 3) suggested that the decreased ability of *mdm10*Δ and *mdm12*Δ cells to respire may be associated with their defective mitochondrial morphology, while the fully respiratory competent *mdm34*Δ exhibited near-normal morphology. Moreover, these results indicate that the resistance to acetic acid shown by *mdm34*Δ cells is not a consequence of respiratory inability. Equivalent phenotypes were also encountered after growing all strains at a non-permissive temperature (Fig. 6a, left panel).

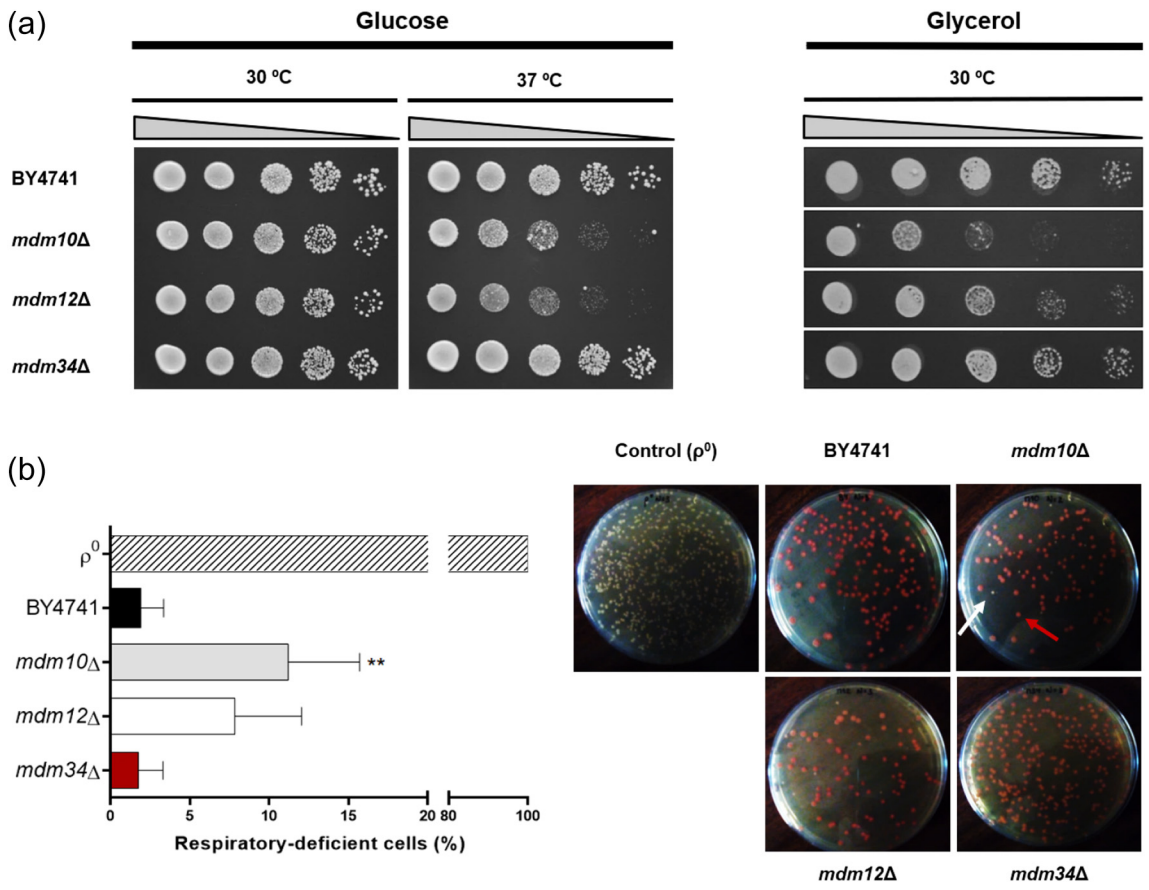

Fig. 6. Yeast cells lacking ERMES complex components display different temperature sensitivity, respiratory ability and *petite* induction. (a) Left panel: Drop dilution assays were performed on two YEPDA plates, with one being incubated at 30 °C and the other at 37 °C for 48 h. Right panel: For evaluation of growth on a non-fermentable carbon source, drop dilution assays were performed on SC Glycerol plates, which were incubated at 30 °C for 72 h. Data represent one of three independent experiments. (b) Lack of *MDM10* promotes petite formation in *S. cerevisiae*. YEPG-grown wild-type and mutant strains were spread onto YEPDA plates and allowed to grow for 96 h. Loss of respiratory function was assessed by the tetrazolium assay [62]. Actively respiring colonies are able to reduce the compound and gain a red tonality (red arrow), while respiratory-deficient cells remain white (white arrow). A respiratory-deficient (ρ^0) strain was used as positive control. Scoring was performed after 3 h and confirmed again after 72 h of tetrazolium overlay. Reported values represent the mean ± SD of three independent experiments (one-way ANOVA, Dunnett's *post hoc* test: $^{**}p < 0.01$).

Of note, more than a decrease in colony number we rather observed a drastic reduction in colony size on both assays with *mdm10*Δ and *mdm12*Δ strains. Since loss of mtDNA is one of the causes for *petite* formation and the ERMES complex has been linked to the anchoring of mtDNA nucleoids and mtDNA replication [45–47], we evaluated the rate at which ERMES-deficient cells lost their respiratory capacity by measuring the appearance of colonies with a *petite* phenotype. For this purpose, wild-type and mutant strains were subjected to the tetrazolium overlay assay [66]. White colonies (unable to reduce tetrazolium) were scored as *petite* and red colonies as respiratory competent (Fig. 6b). In agreement with our results regarding respiratory ability and temperature sensitivity, we observed that *mdm34*Δ cells exhibited a similar phenotype in comparison to the wild-type strain, with petite induction percentages of 1.78% ± 1.27% and 1.74% ± 1.27%, respectively. Not surprisingly, the *mdm10*Δ and *mdm12*Δ strains displayed a higher loss of respiratory ability with 11.2% ± 3.7% and 7.8% ± 3.4% of colonies remaining white after 3 h. To ensure proper white/red screening, we repeated the scoring process after 72 h and observed no differences in the results.

Aiming to investigate if the resistance phenotype we encountered after acetic acid challenge could be due to an unspecific hindrance of the mutants to commit to a cell death program, we evaluated if ERMES deficiency could impact the overall life span of *S. cerevisiae*. For that purpose, we evaluated chronological aging through assessment of clonogenic survival during a 17-day period. Our results indicate that cells lacking the ERMES complex are more prone to lose viability than

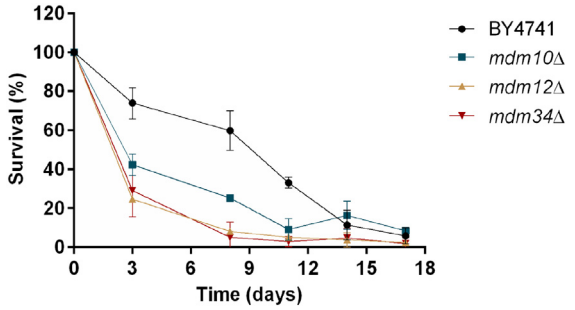

Fig. 7. Ablation of ERMES complex components reduces the chronological life span of *S. cerevisiae*. Wild-type and mutant strains were grown in SC glucose media to stationary phase for 3 days, by the end of which the first samples were collected (time 0). The experiment was carried out for 17 days and survival was evaluated by CFU counts on YEPDA plates. Time 0 was considered 100% of viability. Results are expressed as mean ± SD of three (BY4741 and *mdm34*Δ) or two (*mdm10*Δ and *mdm12*Δ) independent experiments.

the wild-type strain, indicating that the resistance shown is specific for acetic acid (Fig. 7).

ERMES components mediate cytochrome *c* release upon acetic acid treatment

Cytochrome *c* release from mitochondria is a known hallmark of both mammalian and yeast apoptosis [18,67]. To test our initial hypothesis that ERMES could mediate the release of pro-apoptotic proteins to the cytosol, we evaluated cytochrome *c* release from mitochondria. In order to do so, a change of carbon source was required since glucose is a repressor of mitochondrial respiration and therefore mitochondrial mass is scarce [68]. As such, we changed the carbon source to galactose which is a weaker repressor of mitochondrial respiration and would thus allow a higher mitochondrial cytochrome *c* content [69].

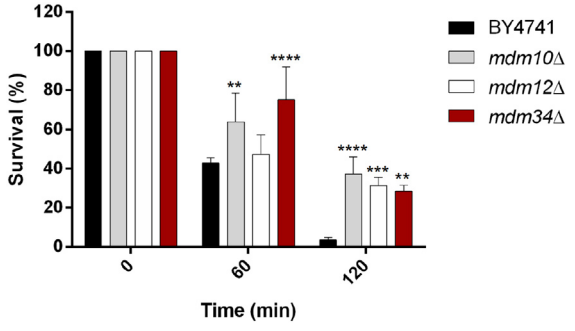

Fig. 8. Absence of ERMES complex components induces resistance to acetic acid treatment in galactose medium. Wild-type and mutant strains were grown to exponential phase in YEPGal media and shifted to YEPGal (pH 3.0) media before 100 mM acetic acid treatment for 200 min. Clonogenic survival was evaluated by CFU counts on YEPDA plates, where time 0 was considered 100% of viability. The results are expressed as mean ± SD of three independent experiments (two-way ANOVA, Dunnett's *post hoc* test: $^{**}p < 0.01$, $^{***}p < 0.001$, $^{****}p < 0.0001$).

To ensure that the resistance to acetic acid was not affected by the change in medium composition, we performed clonogenic survival assays in galactose medium (Fig. 8). Although all strains were still significantly resistant to acetic acid challenge under these conditions, the resistance shown by *mdm34*Δ cells was considerably decreased in galactose in comparison to glucose medium. Considering that one difference between both carbon sources is that respiration is less inhibited by galactose, we sought to determine if by inhibiting respiration the strains could revert to the original phenotype. A 1-h pre-incubation period with complex III and V inhibitors antimycin A and oligomycin, respectively, did not alter cell survival in galactose medium, although respiration was blocked, as measured by Clarke electrode (data not shown). As such, the decrease in resistance of *mdm34*Δ cells to acetic acid in galactose medium does not appear to be dependent on mitochondrial respiration.

For the evaluation of cytochrome *c* release, untreated and treated cells were subjected to mitochondria fractionation. Mitochondrial cytochrome *c* content was assessed by Western blot analysis, and the extent of release was measured by band intensity normalized to the respective loading control (Fig. 9). The results clearly demonstrate that the absence of certain ERMES complex components has an impact on cytochrome *c* release. Notably, we found that absence of either Mdm10p or Mdm34p prevented the release of cytochrome *c* from mitochondria almost completely, with Cyc1p/Por1p relative ratios of 1.07 ± 0.07 and 0.92 ± 0.04, respectively, in comparison to untreated samples. On the other hand, both wild-type and *mdm12*Δ strains exhibited a high degree of cytochrome *c* release from mitochondria after acetic acid treatment.

Absence of ERMES alters the mitochondrial phospholipidic profile of *S. cerevisiae*

Considering the putative role of the ERMES complex in lipid traffic and the role of some phospholipids such as cardiolipin (CL) and phosphatidylserine (PS) in apoptosis [70,71], we next assessed if mutants presented basal alterations in mitochondrial phospholipid composition that could account for the resistance shown. Mitochondrial fractions from untreated samples used to assess cytochrome *c* release were subjected to phospholipid analysis (Fig. 10a). All mutants exhibited a significant increase in phosphatidylethanolamine (PE) content in relation to the wild-type strain, since although phosphatidylglycerol (PG) co-migrates with PE, its contribution to the global phospholipidic content is very low [72,73]. PG is also the CL precursor, so it is unlikely that PG levels were considerably increased since CL levels were identical in the wild-type and mutant strains. On the other hand,

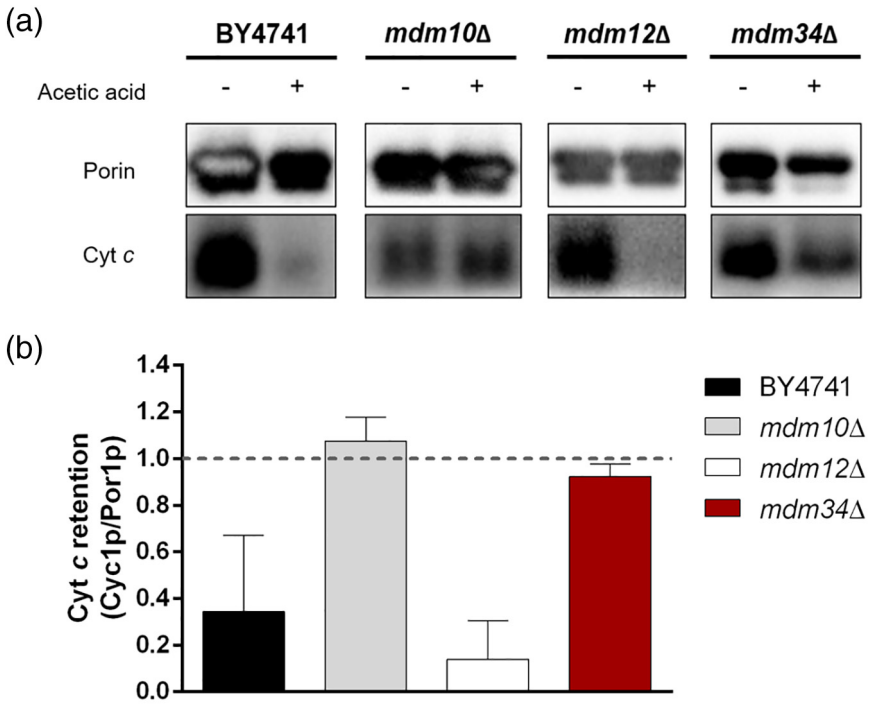

Fig. 9. Cytochrome *c* release after acetic acid challenge is abrogated in cells lacking either Mdm10p or Mdm34p. Wild-type and mutant strains were subjected to mitochondrial fractionation in YEPGal pH 3.0 medium before (–) and after (+) exposure to 100 mM acetic acid treatment. (a) Mitochondrial cytochrome *c* (Cyc1p) content was evaluated by Western blot analysis. Mitochondrial porin (Por1p) was used as loading control. A representative experiment is shown for each strain out of two independent experiments. (b) Protein levels on mitochondrial fractions before and after treatment were quantified by band intensity using the ImageJ software. Cytochrome *c* levels after treatment were normalized to the corresponding loading control and to the respective ratio of untreated cells. Values are the mean ± SD of two independent experiments. Dashed gray line represents a Cytochrome *c*/Porin ratio of 1, meaning no cytochrome *c* was released.

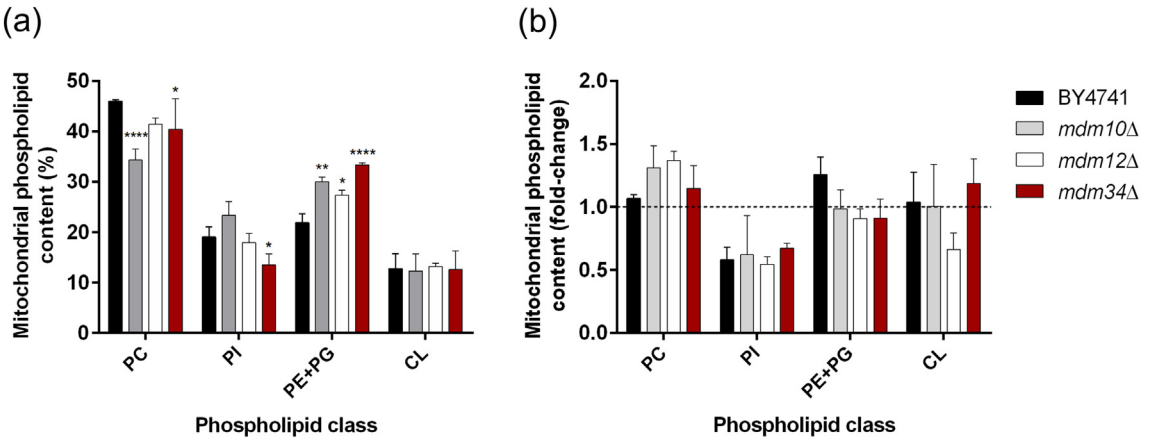

Fig. 10. Phospholipid analysis of mitochondria from wild-type and ERMES-deficient cells. Mitochondrial fractions of untreated wild-type and mutant strains were subjected to phospholipid quantification. Lipid extraction was performed through the Bligh and Dyer method, and quantification of phospholipid classes was assessed by phosphorus measurement after TLC separation. (a) Cells lacking the ERMES complex exhibit an altered mitochondrial phospholipidic profile. (b) ERMES-mediated lipid exchange function is not impaired after acetic acid challenge. Results are expressed as mean ± SD of three independent experiments (two-way ANOVA, Dunnett's *post hoc* test: $*p < 0.05$, $**p < 0.01$, $****p < 0.0001$). PC, phosphatidylcholine; PI, phosphatidylinositol; PE, phosphatidylethanolamine; PG, phosphatidylglycerol; CL, cardiolipin.

both *mdm10*Δ and *mdm34*Δ exhibited a decrease in the phosphatidylcholine (PC) class. No noteworthy differences were found neither for phosphatidylinositol (PI) nor for CL levels.

To further infer if the resistance shown by ERMES mutants to acetic acid treatment involved ERMES-mediated lipid transfer, we analyzed the mitochondrial phospholipid content of acetic acid-treated cells (Fig. 10b). Since ERMES mutants already display an altered phospholipidic profile, we assessed the fold-change of relative percentages after acetic acid treatment. The results showed that mitochondria of both wild-type and mutant strains undergo similar alterations in terms of phospholipid content, with a significant reduction of PI content in all strains.

Discussion

The involvement of ER-MCS in disease has been previously attested for in pathologies such as neurodegenerative diseases and cancer [74–79]. Interestingly, these diseases are also characterized by dysregulated apoptosis. In this context, the possible involvement of ER-MCS in cell death has been the subject of recent interest. While there are some studies linking ER-MCS with mammalian apoptosis, to the extent of our knowledge, no experimental data have been put forward evidencing a role of ER-MCS in mammalian MOMP or of the ERMES complex in yeast MOMP and regulated cell death.

Our initial analysis on clonogenic survival after acetic acid challenge demonstrated that yeast cells deficient in ERMES complex components exhibit a resistance phenotype to this stressor, therefore establishing a starting point for a putative role of these proteins in acetic acid-induced apoptosis. A general resistance to cell death was not intrinsically acquired upon mutation, since ablation of Mdm12p, Mdm10p or Mdm34p reduced the chronological life span of *S. cerevisiae*. The similar shortening of chronological longevity in these strains suggests that this could be attributed to the loss of a common function, namely, the one carried out by ERMES. In fact, there have been reports that ablation of any of the ERMES components leads to the disruption of the whole complex [40]. Thus, it should be borne in mind that by evaluating the phenotype of each deletion mutant we may be ascertaining either a direct or indirect role of the deleted protein, that is, the role of the protein or the role of the whole complex, respectively. Indeed, it is interesting that the three deletion mutants do not exhibit similar survival percentages upon acetic acid treatment, as it would be expected if the complex itself was the sole responsible for resistance. Instead, *mdm34*Δ cells are extremely resistant to acetic acid challenge in glucose media, while *mdm10*Δ and *mdm12*Δ viability is more affected, though still resistant.

The interpretation that the mutant's resistance phenotype is a consequence of a protein-specific function rather than ERMES complex disruption was further supported by the delayed emergence of several death markers during acetic acid treatment. Indeed, the extent of the loss of plasma membrane integrity in *mdm34*Δ cells was much lower than that of *mdm10*Δ and *mdm12*Δ. Furthermore, *mdm10*Δ and *mdm12*Δ cells display a transient hyperpolarization similarly to the wild-type strain (although delayed), whereas *mdm34*Δ mitochondria are unable to hyperpolarize to an equivalent degree. Also, the mutant strains reveal a significant difference in the accumulation of superoxide anion in comparison to the wild-type, more prominently in *mdm34*Δ than in *mdm10*Δ or *mdm12*Δ. Mitochondrial degradation of cells deficient in ERMES components is one of the most noteworthy hallmarks studied, with all mutants displaying a pronounced decrease in mitochondrial degradation in comparison to the wild-type strain. Thus, it seems that although these mutants are able to resist acetic acid challenge in different degrees, the similar mitochondrial degradation profile indicates a possible role of the whole complex in this process. Pep4p, a vacuole protease that is released from the vacuole to the cytosol upon acetic acid treatment, is thought to mediate the mitochondrial degradation process [26]. As such, it is possible that Pep4p and ERMES interact to promote mitochondrial degradation. Impairment of cytochrome *c* release from mitochondria after acetic acid challenge is also an impressive feature of *mdm10*Δ and *mdm34*Δ strains in contrast with both wild-type and *mdm12*Δ. These results corroborate our initial premise that the ERMES complex, namely its MOM components, is required for cytochrome *c* release. Of note, acetic acid-induced apoptosis could also occur without cytochrome *c* release, although delayed, as previously described [25,80].

In agreement with previous reports, cells lacking ERMES complex components display impaired growth on non-fermentable carbon sources [40,64,65]. This feature appeared to correlate with mitochondrial morphology since *mdm10*Δ and *mdm12*Δ, which fail (to some extent) to grow on glycerol plates, are actually the ones displaying an abnormal mitochondrial morphotype. Notwithstanding, *mdm34*Δ cells do not exhibit giant mitochondria or impaired growth on non-fermentable media. Therefore, although these phenotypes may have a causal relationship, *mdm34*Δ resistance to acetic acid is not due to any of these features. Importantly, the near-normal mitochondrial morphology and respiratory ability of cells lacking Mdm34p may also translate into a higher resistance to acetic acid treatment through the maintenance of a stronger antioxidative environment, thus explaining the lower accumulation of superoxide anion [81].

Overall, these results hint that each protein must also exert other functions besides their role in ERMES. In fact, Mdm10p has a role on the sorting

and assembly machinery (SAM), a protein complex that mediates the insertion of β-barrel proteins into the MOM. The SAM complex and Mdm10p are thought to play a role in the maturation of the TOM complex [82,83]. Interestingly, this complex has been deemed as required for Bax-induced cytochrome *c* release [84], although this subject has been disputed [85]. Thus, ablation of Mdm10p carries pleiotropic effects that could be masking the role of the ERMES complex in acetic acid-induced apoptosis, accounting for the difference in viability between *mdm10*Δ and *mdm34*Δ cells, although both show impairment in cytochrome *c* release. Considering that Mdm12p does not appear to have a role in cytochrome *c* release, it is likely that the resistance shown by *mdm12*Δ cells stems from disruption of ERMES function.

Ascribed functions of ERMES encompass phospholipid and calcium traffic between the ER and the MOM. Calcium is a known signaling molecule of cell death in metazoans, where it is mobilized from the ER to mitochondria through ER-MCS [57,86]. Likewise, phospholipids such as PS and CL have already been implicated in both mammalian and yeast apoptosis [70,71,87]. Thus, it is possible that these functions could modulate the yeast response to acetic acid and, at least in part, explain the acquired resistance of all mutants. Our results regarding mitochondrial phospholipid composition revealed that cells lacking the ERMES complex components Mdm10p, Mdm12p or Mdm34p exhibit an increase in mitochondrial PE, while absence of Mdm10p or Mdm34p also results in a decrease of mitochondrial PC (Fig. 10a). As with chronological life span and mitochondrial degradation, the altered phospholipid composition of mitochondria also appears to be a consequence of ER–mitochondria untethering rather the loss of a protein-specific function. A thorough literature search revealed that some studies are in agreement with our results, whereas others do not comply with our data. In the latter case, a reduction of both mitochondrial PE and CL levels and increase in PS content were reported [40,88–91]. The difference between results could be attributed to the use of different genetic backgrounds (all of them), growth conditions [88,90,91] or method of analysis [65,88,89]. On the other hand, ERMES complex disruption has been shown to reduce the PS to PC conversion rate [40] but not PS to PE [43,92], or PS transfer from the ER to mitochondria [93]. These results agree with our own, since we only detected an increase in mitochondrial PE and reduced PC content. Moreover, it has been hypothesized that different ER–mitochondria tethering complexes could be responsible for distinct types of transport [93]. Indeed, our results corroborate a recent model where ERMES may mainly mediate PE transport from mitochondria to the ER [94]. In light of this, PE would accumulate in mitochondria and diminish ER-mediated PC synthesis, which could subsequently impair its transport back to mitochondria. In agreement, Mdm12p has recently been found to preferentially bind to phospholipids carrying a positively charged head group, that is, PE and PC [95]. In what pertains to cell death, it was found that substitution of lamellar PC for non-lamellar PE in a lipid bilayer introduces a mechanical pressure in the hydrocarbon region of the membrane that is able to modulate VDAC gating properties, with non-lamellar lipids stabilizing the closed state of VDAC [96]. Considering that Por1p has a protective role in acetic acid-induced apoptosis [25], potentially by acting on Aac1/2/3-dependent cytochrome *c* release [29], ERMES could also modulate Por1p conformation by altering mitochondrial phospholipid composition and stabilizing its closed state.

Importantly, mitochondrial PE was found to regulate mitochondrial function and morphology, while ER-synthesized PE appears to be required for cell growth [97]. Together with our results, this indicates that mitochondrial dysfunction and morphology of both *mdm10*Δ and *mdm12*Δ strains is not due to a reduced mitochondrial PE synthesis. Moreover, PE is reported to extend chronological life span through autophagy induction [98]. This phenotype is not encountered for our mutant strains that, although having an increased mitochondrial PE content, display a shorter chronological life span. Moreover, the higher survival of ERMES-deficient strains to cell death is not due to autophagy induction since this process is absent in cells undergoing acetic acid treatment [25].

We also assessed if the lipid exchange function of ERMES could potentially contribute to the resistance shown by ERMES-deleted strains to acetic acid. However, no noteworthy differences were found between wild-type and mutant strains based on the fold-change of phospholipid content after treatment (Fig. 10b), suggesting that ERMES-mediated lipid transport from ER to mitochondria is not involved in acetic acid-induced apoptosis. Strikingly, all strains revealed a significant decrease in mitochondrial PI content, pointing to a possible role of this phospholipid in cell death induced by this stressor. In line with this interpretation, it was found that a decrease in mitochondrial PI(4,5)bisphosphate content induces mitochondrial fragmentation in mammalian cells, a common apoptotic event also observed in acetic acid-induced apoptosis [99].

In addition, acetic acid has been recently shown to induce ER stress and activation of the unfolded protein response [100]. When this pathway fails to cope with protein misfolding, cell death is induced by exchanging signals with mitochondria that result in the activation of apoptosis [101]. Hence, it could be that the ERMES complex is the signaling hub responsible for signal exchange during acetic acid-induced ER stress, which would also partially explain the phenotypes encountered.

In conclusion, we report experimental evidence for a role of the ERMES complex in acetic acid-induced

apoptosis. Through the use of single deletion mutants, we were able to determine a delay in the emergence of several apoptotic hallmarks, including an impairment of cytochrome *c* release in strains lacking either one of the two MOM proteins of the ERMES complex. With this work, we identify the ERMES components Mdm10p and Mdm34p as new players of the molecular machinery that promotes cytochrome *c* release in yeast apoptosis induced by acetic acid.

Materials and Methods

Yeast strains and plasmids

S. cerevisiae BY4741 (*MATa his3Δ1 leu2Δ0 met15Δ0 ura3Δ0*) was used as the wild-type strain. This and all mutant strains (*mdm10*Δ, *mdm12*Δ and *mdm34*Δ) belong to the haploid mutant knockout collection from EUROSCARF (Frankfurt, Germany) and were generated through insertion of a kanamycin cassette (*KanMX4*) within the target gene [102]. Confirmation of correct *KanMX4* insertion was achieved by PCR using primers that bind upstream and downstream of the target gene as well as within *KanMX4*, followed by agarose gel electrophoresis (Table 1). All strains were also transformed with a plasmid encoding a mitochondrial matrix-targeted green fluorescent protein (pYX242-mtGFP, *LEU2*) by the lithium/acetate method [103]. Selection of positive transformants was performed through auxotrophic selection in media lacking leucine and validated by fluorescence microscopy. Strain BY4741 ρ^0 (lacking mtDNA) was kindly provided by Flávia Sousa (Center of Molecular and Environmental Biology, University of Minho, Portugal).

Growth conditions and media composition

Yeast strains were grown in liquid YEP medium [1% (w/v) yeast extract, 2% (w/v) peptone] supplemented with the appropriate carbon sources [YEPD: 2% (w/v) glucose; YEPG: 2% (v/v) glycerol; YEPGal: 2% (w/v) galactose] and maintained on solid YEPDA plates [YEPD plus 2% (w/v) agar]. For assessment of respiratory ability, strains were grown in solid selective complete medium [SC; 0.17% (w/v) yeast nitrogen base without amino acids or ammonium sulfate, 0.5% (w/v) ammonium sulfate, 0.2% (w/v) amino acid drop-out mix, 0.01% appropriate auxotrophic requirements] with 2% (w/v) glycerol and 2% (w/v) agar. Yeast strains carrying pYX424-mtGFP were selected and grown in SC medium with 2% glucose lacking leucine (SC Glu -Leu).

Acetic acid treatment and survival assays

Strains were cultured overnight in YEPD or YEPGal medium until the exponential growth phase was reached ($OD_{640\ nm}$ = 0.6–0.8). Cells were then harvested and resuspended in the same medium at pH 3.0 (set with HCl), treated with 100 mM acetic acid (Panreac) and incubated under the same conditions for up to 200 min. At this particular pH, approximately 82.6% of acetic acid (p*K*a = 4.76) is in its undissociated form. For survival assays, a sample yielding approximately 10^7 cells was collected at specific time points (0, 60, 120, 180 or 200 min), serial diluted and spotted on YEPDA plates. After incubation for 48 h at 30 °C, colony forming units (CFU) were counted. For chronological aging assays, strains were grown in SC media with 2% (w/v) glucose for 72 h. Afterward, samples were serial diluted and spotted on YEPDA plates, and CFU were counted after 48 h of growth at 30 °C. This was considered to be the time 0 of the experiment. Sampling was repeated periodically for 17 days.

Flow cytometry

Flow cytometry analysis was performed in an Epics® XL-MCL™ (Beckman COULTER®) flow cytometer equipped with an argon ion laser emitting a 488-nm beam at 15 mW. All strains were grown and treated as described above. At each time point, cells were harvested, washed and suspended in proper media to a final concentration of 10^6 cells/mL. For PI (Sigma-Aldrich) or DHE (Sigma-Aldrich) staining, cells were suspended in phosphate-buffered saline and incubated with either 1 μg/mL PI for 10 min or 2 μg/mL DHE for 20 min at room temperature in the dark. Monoparametric detection of PI and DHE fluorescence was achieved by collecting red fluorescence through a 675-nm band-pass filter (FL-4 channel). For assessment of $\Delta\Psi_m$, cells were suspended in MES buffer [10 mM MES (2-(*N*-morpholino)ethanesulfonic acid); 0.1 mM $MgCl_2$; 2% (w/v) glucose, pH 6 adjusted with $Ca(OH)_2$] and co-stained with 1 nM 3,3′-dihexyloxacarbocyanine iodide [$DiOC_6(3)$; Thermo Fisher Scientific] for 30 min at 30 °C in the dark, and 1 μg/mL PI 10 min prior to analysis. For mitochondrial degradation assays, cells carrying pYX242-mtGFP were suspended in

Table 1. List of primers used for *KanMX4* confirmation

Strain	Forward primer (5′–3′)	Reverse primer (5′–3′)
*mdm10*Δ	CTGGCTCCATGACCTCCTT	GATGAAGCTTTGAGCGAAAGT
*mdm12*Δ	TCAATGTCTGTGAGGGCCTTAT	ACGGACAACTGTCTAGAGTATGAGAT
*mdm34*Δ	GGGCCATGAAGCCTTGTAG	TCATGCCTTTAGCTGCAAGT

phosphate-buffered saline and immediately analyzed. Monoparametric detection of $DiOC_6(3)$ and GFP fluorescence was attained through a 525-nm band-pass (FL1-channel), and fluorescence was normalized to cell size to eliminate fluorescence variations due to cellular volume. In addition, for mitochondrial degradation, the FL1 peak was used as a quantitative parameter for the integrity of mitochondrial networks by discriminating between spots of intense mitochondrial GFP signal and diffuse cytoplasmic GFP resultant from mitochondrial degradation. For all assays, approximately 30,000 cells were analyzed per sample and data were analyzed using FlowJo X 10.0.7r2 software.

Fluorescence microscopy

An automated Leica Microsystems DM-5000B epifluorescence microscope coupled to a Leica DCF350 FXR2-193510309 digital camera was used to assess mitochondrial morphology. All strains carrying pYX242-mtGFP were grown in SC Glu -Leu to an $OD_{640\ nm}$ = 0.8, and samples were transferred to glass slides, mounted carefully with a coverslip and quickly visualized. Photomicrographs were acquired and processed using Leica Application Suite (LAS) AF 6000 LX Microsystems software with a 100× oil immersion objective lens with numerical aperture of 1.3 and 1.6× magnification change. For each cell analyzed, images were taken using appropriate filter settings for differential phase contrast and green fluorescence (GFP). The produced photomicrographs were further managed with the LAS X v. 3.3.0.16799, GIMP v.2.8.22 and ImageJ v. 1.51j8 software.

Respiratory ability, temperature sensitivity and *petite* induction

Wild-type and mutant strains were grown in YEPD medium until an $OD_{640\ nm}$ of 1.5 and serial diluted. For the assessment of respiratory capacity, drops of all dilutions were spotted on SC Glycerol plates and incubated for 72 h at 30 °C. For evaluation of temperature sensitivity, drops of all dilutions were spotted on YEPDA plates and simultaneously allowed to grow for 48 h at 30 °C or 37 °C. For monitoring *petite* induction, strains were grown overnight in YEPG medium to an $OD_{640\ nm}$ of 1.5 and then serial diluted. Drops from the 10^{-4} dilution were spotted on YEPDA plates and homogeneously spread with 1-mm glass beads. After growth for 96 h at 30 °C, assessment of respiratory-competent colonies was performed by the tetrazolium overlay technique [66].

Mitochondrial fractionation and protein extraction

For mitochondria isolation, wild-type and mutant strains were cultured overnight on YEPGal medium in 3-L flasks with a flask/medium volume ratio of 5:1 until an $OD_{640\ nm}$ = 1.5–1.8. For each experiment, 1.2 L of culture was harvested, washed and incubated in YEPGal medium (pH 3.0) in the absence or presence of 100 mM acetic acid. Incubation time of wild-type and mutant strains was 60 and 90 min, respectively. Mitochondria fractionation was performed as previously described [104], with only one alteration: 10 mg of Zymolyase-20T (GRiSP Research Solutions) was added per gram of non-treated cells and 20 mg per gram of acetic acid-treated cells. Protein concentration was determined through the Bradford method [105] in a Varian Carry 50® UV–Visible spectrophotometer. Approximately 75 μg of protein from mitochondrial fractions was precipitated as previously described [25].

Western blot analysis

Protein samples from isolated mitochondrial fractions were separated by SDS 12.5% polyacrylamide gel electrophoresis as described elsewhere [25]. Proteins were transferred from the gels to polyvinylidene fluoride membranes (Amersham Hybond-P; GE Healthcare Life Sciences) using a Semi-dry TE77X Transfer Unit (Hoefer). Primary antibodies used were rabbit polyclonal anti-yeast cytochrome *c* (1:1000, custom-made by Millegen) and mouse monoclonal anti-yeast porin (1:5000; Invitrogen). Immunodetection was achieved by chemiluminescence using the ECL detection system (Merck Millipore) and visualized in a ChemiDoc XRS Imaging System (Bio-Rad). Derivatizations of protein content by band intensity were performed using the ImageJ v. 1.51j8 software.

Lipid extraction, phospholipid quantification and thin-layer chromatography

Lipids were extracted from mitochondrial suspensions according to Bligh and Dyer method [106] and as previously described by our laboratory [107]. The amount of phospholipids after extraction was quantified with the phosphorus assay as described by Bartlett and Lewis [108]. Briefly, samples were dissolved in $CHCl_3$, after which 70% (w/v) perchloric acid was added to an aliquot of 10 μL. The mixture was heated at 180 °C for 1 h and cooled at room temperature. Afterward, ammonium molybdate and ascorbic acid were added to the samples to a final concentration of 0.3 and 10% (w/v) in Mili-Q water, respectively. The reaction mixture was incubated for 10 min at 100 °C in a water bath and cooled on water. Standards from 0.1 to 2 μg of phosphate underwent the same treatment with exception of the heating block phase. Finally, samples were added to 96-multiwell plates, and absorbance was measured at 797 nm. The amount of phosphorus present in each sample was calculated by linear regression [109]. Phospholipid class separation was achieved by thin-layer

chromatography (TLC). Prior to separation, TLC plates were washed in a TLC chamber with a methanol/chloroform mixture (1:1, v/v) for 15 min. The plates were then sprayed with 2.3% (w/v) boric acid and dried in an oven at 100 °C for 15 min. For the separation of the phospholipid classes, a volume equivalent to 30 μg of phospholipids was applied on the TLC plates. The plates were dried with nitrogen flow and developed with chloroform/ethanol/water/triethylamine (30:35:7:35, v/v/v/v). Lipid spots were identified by spraying the plate with 0.5 μg/mL primuline solution dissolved in acetone/Mili-Q water (80:20, v/v), and visualized with a UV lamp (λ = 254 nm). Phospholipid classes were identified by comparison with standards, scraped from the TLC plates and quantified by the phosphorus assay as described above.

Statistical analysis

Reported data are expressed as mean ± SD of independent experiments. Statistical analysis was performed on GraphPad Prism v. 6.01 (GraphPad Software Inc., La Jolla California USA). One-way (Fig. 6) and two-way (Figs. 1, 4, 5 and 8) analysis of variance (ANOVA) tests were performed followed by Dunnet's *post hoc* test for multiple comparisons between wild-type (BY4741) and mutant strains. Significance was considered whenever $p < 0.05$.

Acknowledgments

The authors wish to thank Stéphen Manon for providing the anti-cytochrome *c* antibody and Clara Pereira for providing the pYX232-mtGFP plasmid. This work was funded by the strategic program UID/BIA/04050/2013 (POCI-01-0145-FEDER-007569) financed by national funds through Fundação para a Ciência e a Tecnologia (FCT) and by Fundo Europeu de Desenvolvimento Regional (FEDER) through COMPETE 2020–Programa Operacional Competitividade e Internacionalização (POCI).

Declarations of Interest: None.

Received 9 August 2018;
Received in revised form 12 October 2018;
Accepted 5 November 2018
Available online 8 November 2018

Keywords:
yeast cell death;
weak acid;
mitochondrial outer membrane permeabilization;
membrane contact sites

Present address: T.R. Fernandes, Departamento de Genética, Universidad de Córdoba, Córdoba, Spain.

Present address: C.B. Afonso, School of Life and Health Sciences, Aston Triangle, Aston University, Birmingham, United Kingdom.

Abbreviations used:
ER-MCS, endoplasmic reticulum–mitochondria contact sites; ERMES, ER–mitochondria encounter structure; MOM, mitochondrial outer membrane; MOMP, MOM permeabilization; mPTP, mitochondrial permeability transition pore; mtDNA, mitochondrial DNA; mtGFP, mitochondrial GFP.

References

[1] G. Kroemer, L. Galluzzi, P. Vandenabeele, J. Abrams, E. Alnemri, E. Baehrecke, M. Blagosklonny, W. El-Deiry, P. Golstein, D. Green, M. Hengartner, R. Knight, S. Kumar, S.A. Lipton, W. Malorni, G. Nuñez, M. Peter, J. Tschopp, J. Yuan, M. Piacentini, B. Zhivotovsky, G. Melino, Classification of cell death: recommendations of the Nomenclature Committee on Cell Death 2009, Cell Death Differ. 16 (2009) 3–11.

[2] A.P. Halestrap, G.P. McStay, S.J. Clarke, The permeability transition pore complex: another view, Biochimie 84 (2002) 153–166.

[3] K.W. Kinnally, B. Antonsson, A tale of two mitochondrial channels, MAC and PTP, in apoptosis, Apoptosis 12 (2007) 857–868.

[4] P. Bernardi, F. Di Lisa, The mitochondrial permeability transition pore: molecular nature and role as a target in cardioprotection, J. Mol. Cell. Cardiol. 78 (2015) 100–106.

[5] C.P. Baines, R.A. Kaiser, N.H. Purcell, N.S. Blair, H. Osinska, M.A. Hambleton, E.W. Brunskill, M.R. Sayen, R.A. Gottlieb, G.W. Dorn, J. Robbins, J.D. Molkentin, Loss of cyclophilin D reveals a critical role for mitochondrial permeability transition in cell death, Nature 434 (2005) 658–662.

[6] C.P. Baines, R.A. Kaiser, T. Sheiko, W.J. Craigen, D. Molkentin, Voltage-dependent anion channels are dispensable for mitochondrial-dependent cell death, Nat. Cell Biol. 9 (2007) 550–555.

[7] J. He, H.C. Ford, J. Carroll, S. Ding, I.M. Fearnley, J.E. Walker, Persistence of the mitochondrial permeability transition in the absence of subunit c of human ATP synthase, Proc. Natl. Acad. Sci. 114 (2017) 3409–3414.

[8] K. Herick, R. Krämer, H. Lühring, Patch clamp investigation into the phosphate carrier from *Saccharomyces cerevisiae* mitochondria, Biochim. Biophys. Acta 1321 (1997) 207–220.

[9] J.E. Kokoszka, K.G. Waymire, S.E. Levy, J.E. Sligh, J. Cai, D.P. Jones, G.R. Macgregor, D.C. Wallace, The ADP/ATP translocator is not essential for the mitochondrial permeability transition pore, Nature 427 (2004) 461–465.

[10] J.Q. Kwong, J. Davis, C.P. Baines, M.A. Sargent, J. Karch, X. Wang, T. Huang, J.D. Molkentin, Genetic deletion of the mitochondrial phosphate carrier desensitizes the mitochondrial permeability transition pore and causes cardiomyopathy, Cell Death Differ. 21 (2014) 1209–1217.

[11] T. Nakagawa, S. Shimizu, T. Watanabe, O. Yamaguchi, K. Otsu, H. Yamagata, H. Inohara, T. Kubo, Y. Tsujimoto, Cyclophilin D-dependent mitochondrial permeability transition regulates some necrotic but not apoptotic cell death, Nature 434 (2005) 652–658.

[12] J. Šileikytė, E. Blachly-Dyson, R. Sewell, A. Carpi, R. Menabò, F. Di Lisa, F. Ricchelli, P. Bernardi, M. Forte, Regulation of the

mitochondrial permeability transition pore by the outer membrane does not involve the peripheral benzodiazepine receptor (translocator protein of 18 kDa (TSPO))*, J. Biol. Chem. 289 (2014) 13769–13781.
[13] W. Zhou, F. Marinelli, C. Nief, Atomistic simulations indicate the c-subunit ring of the F_1F_O ATP synthase is not the mitochondrial permeability transition pore, elife 6 (2017) 1–11.
[14] L.M. Dejean, S. Martinez-Caballero, S. Manon, K.W. Kinnally, Regulation of the mitochondrial apoptosis-induced channel, MAC, by BCL-2 family proteins, Biochim. Biophys. Acta 1762 (2006) 191–201.
[15] E.V. Pavlov, M. Priault, D. Pietkiewicz, E.H.Y. Cheng, B. Antonsson, S. Manon, S.J. Korsmeyer, C.A. Mannella, K.W. Kinnally, A novel, high conductance channel of mitochondria linked to apoptosis in mammalian cells and Bax expression in yeast, J. Cell Biol. 155 (2001) 725–731.
[16] S.W.G. Tait, D.R. Green, Mitochondria and cell death: outer membrane permeabilization and beyond, Nat. Rev. Mol. Cell Biol. 11 (2010) 621–632.
[17] P. Ludovico, M.J. Sousa, M.T. Silva, C. Leão, M. Côrte-Real, *Saccharomyces cerevisiae* commits to a programmed cell death process in response to acetic acid, Microbiology 147 (2001) 2409–2415.
[18] P. Ludovico, F. Rodrigues, A. Almeida, M.T. Silva, A. Barrientos, M. Côrte-Real, Cytochrome *c* release and mitochondria involvement in programmed cell death induced by acetic acid in *Saccharomyces cerevisiae*, Mol. Biol. Cell 13 (2002) 2598–2606.
[19] S. Büttner, D. Ruli, F.N. Vögtle, L. Galluzzi, B. Moitzi, T. Eisenberg, O. Kepp, L. Habernig, D. Carmona-Gutierrez, P. Rockenfeller, P. Laun, M. Breitenbach, C. Khoury, K.U. Fröhlich, G. Rechberger, C. Meisinger, G. Kroemer, F. Madeo, A yeast BH3-only protein mediates the mitochondrial pathway of apoptosis, EMBO J. 30 (2011) 2779–2792.
[20] B. Almeida, S. Ohlmeier, A.J. Almeida, F. Madeo, C. Leão, F. Rodrigues, P. Ludovico, Yeast protein expression profile during acetic acid-induced apoptosis indicates causal involvement of the TOR pathway, Proteomics 9 (2009) 720–732.
[21] S. Büttner, T. Eisenberg, D. Carmona-Gutierrez, D. Ruli, H. Knauer, C. Ruckenstuhl, C. Sigrist, S. Wissing, M. Kollroser, K.U. Fröhlich, S. Sigrist, F. Madeo, Endonuclease G regulates budding yeast life and death, Mol. Cell 25 (2007) 233–246.
[22] Y. Cui, S. Zhao, Z. Wu, P. Dai, B. Zhou, Mitochondrial release of the NADH dehydrogenase Ndi1 induces apoptosis in yeast, Mol. Biol. Cell 23 (2012) 4373–4382.
[23] N. Guaragnella, C. Pereira, M.J. Sousa, L. Antonacci, S. Passarella, M. Côrte-Real, E. Marra, S. Giannattasio, YCA1 participates in the acetic acid induced yeast programmed cell death also in a manner unrelated to its caspase-like activity, FEBS Lett. 580 (2006) 6880–6884.
[24] F. Madeo, E. Herker, C. Maldener, S. Wissing, S. Lächelt, M. Herlan, M. Fehr, K. Lauber, S.J. Sigrist, S. Wesselborg, K.U. Fröhlich, A caspase-related protease regulates apoptosis in yeast, Mol. Cell 9 (2002) 911–917.
[25] C. Pereira, N. Camougrand, S. Manon, M.J. Sousa, M. Côrte-Real, ADP/ATP carrier is required for mitochondrial outer membrane permeabilization and cytochrome *c* release in yeast apoptosis, Mol. Microbiol. 66 (2007) 571–582.
[26] C. Pereira, S. Chaves, S. Alves, B. Salin, N. Camougrand, S. Manon, M.J. Sousa, M. Côrte-Real, Mitochondrial degradation in acetic acid-induced yeast apoptosis: the role of Pep4 and the ADP/ATP carrier, Mol. Microbiol. 76 (2010) 1398–1410.
[27] A. Rego, M. Costa, S.R. Chaves, N. Matmati, H. Pereira, M.J. Sousa, P. Moradas-Ferreira, Y.A. Hannun, V. Costa, M. Côrte-Real, Modulation of mitochondrial outer membrane permeabilization and apoptosis by ceramide metabolism, PLoS One 7 (2012).
[28] S. Wissing, P. Ludovico, E. Herker, S. Büttner, S.M. Engelhardt, T. Decker, A. Link, A. Proksch, F. Rodrigues, M. Côrte-Real, K.U. Fröhlich, J. Manns, C. Candé, S.J. Sigrist, G. Kroemer, F. Madeo, An AIF orthologue regulates apoptosis in yeast, J. Cell Biol. 166 (2004) 969–974.
[29] D. Trindade, C. Pereira, S. Chaves, S. Manon, M. Côrte-Real, M. Joao Sousa, VDAC regulates AAC-mediated apoptosis and cytochrome *c* release in yeast, Microb. Cell. 3 (2016) 500–510.
[30] G. Jan, A.S. Belzacq, D. Haouzi, A. Rouault, D. Métivier, G. Kroemer, C. Brenner, Propionibacteria induce apoptosis of colorectal carcinoma cells via short-chain fatty acids acting on mitochondria, Cell Death Differ. 9 (2002) 179–188, https://doi.org/10.1038/sj.cdd.4400935.
[31] S. Ferro, J. Azevedo-Silva, M. Casal, M. Côrte-Real, F. Baltazar, A. Preto, Characterization of acetate transport in colorectal cancer cells and potential therapeutic implications, Oncotarget 7 (2016).
[32] C. Marques, C.S.F. Oliveira, S. Alves, S.R. Chaves, O.P. Coutinho, M. Côrte-Real, A. Preto, Acetate-induced apoptosis in colorectal carcinoma cells involves lysosomal membrane permeabilization and cathepsin D release, Cell Death Dis. 4 (2013) e507.
[33] C.S.F. Oliveira, H. Pereira, S. Alves, L. Castro, F. Baltazar, S.R. Chaves, A. Preto, M. Côrte-Real, Cathepsin D protects colorectal cancer cells from acetate-induced apoptosis through autophagy-independent degradation of damaged mitochondria, Cell Death Dis. 6 (2015) 1–11.
[34] M. Sousa, A.M. Duarte, T.R. Fernandes, S.R. Chaves, A. Pacheco, C. Leao, M. Côrte-Real, M.J. Sousa, Genome-wide identification of genes involved in the positive and negative regulation of acetic acid-induced programmed cell death in *Saccharomyces cerevisiae*, BMC Genomics 14 (2013) 838.
[35] Y. Elbaz, M. Schuldiner, Staying in touch: the molecular era of organelle contact sites, Trends Biochem. Sci. 36 (2011) 616–623.
[36] S. Marchi, S. Patergnani, P. Pinton, The endoplasmic reticulum–mitochondria connection: one touch, multiple functions, Biochim. Biophys. Acta Bioenerg. 1837 (2014) 461–469.
[37] A. Raturi, T. Simmen, Where the endoplasmic reticulum and the mitochondrion tie the knot: the mitochondria-associated membrane (MAM), Biochim. Biophys. Acta, Mol. Cell Res. 1833 (2013) 213–224.
[38] B. Kornmann, The molecular hug between the ER and the mitochondria, Curr. Opin. Cell Biol. 25 (2013) 443–448.
[39] T. Simmen, J.E. Aslan, A.D. Blagoveshchenskaya, L. Thomas, L. Wan, Y. Xiang, S.F. Feliciangeli, C.H. Hung, C.M. Crump, G. Thomas, PACS-2 controls endoplasmic reticulum–mitochondria communication and Bid-mediated apoptosis, EMBO J. 24 (2005) 717–729.
[40] B. Kornmann, E. Currie, S.R. Collins, M. Schuldiner, J. Nunnari, J.S. Weissman, P. Walter, An ER–mitochondria tethering complex revealed by a synthetic biology screen, Science 325 (2009) 477–481.
[41] B. Kornmann, C. Osman, P. Walter, The conserved GTPase Gem1 regulates endoplasmic reticulum–mitochondria connections, Proc. Natl. Acad. Sci. 108 (2011) 14151–14156.
[42] D.A. Stroud, S. Oeljeklaus, S. Wiese, M. Bohnert, U. Lewandrowski, A. Sickmann, B. Guiard, M. Van Der Laan, B. Warscheid, N. Wiedemann, Composition and topology of the endoplasmic reticulum–mitochondria encounter structure, J. Mol. Biol. 413 (2011) 743–750.

[43] T.T. Nguyen, A. Lewandowska, J.Y. Choi, D.F. Markgraf, M. Junker, M. Bilgin, C.S. Ejsing, D.R. Voelker, T.A. Rapoport, J.M. Shaw, Gem1 and ERMES do not directly affect phosphatidylserine transport from ER to mitochondria or mitochondrial inheritance, Traffic 13 (2012) 880–890.
[44] B. Kornmann, P. Walter, ERMES-mediated ER–mitochondria contacts: molecular hubs for the regulation of mitochondrial biology, J. Cell Sci. 123 (2010) 1389–1393.
[45] T. Hanekamp, M.K. Thorsness, I. Rebbapragada, E.M. Fisher, C. Seebart, M.R. Darland, J.A. Coxbill, D.L. Updike, P.E. Thorsness, Maintenance of mitochondrial morphology is linked to maintenance of the mitochondrial genome in *Saccharomyces cerevisiae*, Genetics 162 (2002) 1147–1156.
[46] A.E.A. Hobbs, M. Srinivasan, J.M. McCaffery, R.E. Jensen, Mmm1p, a mitochondrial outer membrane protein, is connected to mitochondrial DNA (mtDNA) nucleoids and required for mtDNA stability, J. Cell Biol. 152 (2001) 401–410.
[47] A. Murley, L.L. Lackner, C. Osman, M. West, G.K. Voeltz, P. Walter, J. Nunnari, ER-associated mitochondrial division links the distribution of mitochondria and mitochondrial DNA in yeast, elife 2013 (2013) 1–16.
[48] S.M. Burgess, M. Delannoy, R.E. Jensen, MMM1 encodes a mitochondrial outer membrane protein essential for establishing and maintaining the structure of yeast mitochondria, J. Cell Biol. 126 (1994) 1375–1391.
[49] C. Meisinger, S. Pfannschmidt, M. Rissler, D. Milenkovic, T. Becker, D. Stojanovski, M.J. Youngman, R.E. Jensen, A. Chacinska, B. Guiard, N. Pfanner, N. Wiedemann, The morphology proteins Mdm12/Mmm1 function in the major β-barrel assembly pathway of mitochondria, EMBO J. 26 (2007) 2229–2239.
[50] S. Böckler, B. Westermann, Mitochondrial ER contacts are crucial for mitophagy in yeast, Dev. Cell 28 (2014) 450–458.
[51] Y. Xue, S. Schmollinger, N. Attar, O.A. Campos, M. Vogelauer, M.F. Carey, S.S. Merchant, S.K. Kurdistani, Endoplasmic reticulum–mitochondria junction is required for iron homeostasis, J. Biol. Chem. 292 (2017) 13197–13204.
[52] I. Boldogh, N. Vojtov, S. Karmon, L.A. Pon, Interaction between mitochondria and the actin cytoskeleton in budding yeast requires two integral mitochondrial outer membrane proteins, Mmm1p and Mdm10p, J. Cell Biol. 141 (1998) 1371–1381.
[53] Y. Hirabayashi, S.-K. Kwon, H. Paek, W.M. Pernice, M.A. Paul, J. Lee, P. Erfani, A. Raczkowski, D.S. Petrey, L.A. Pon, F. Polleux, ER–mitochondria tethering by PDZD8 regulates Ca^{2+} dynamics in mammalian neurons, Science 358 (2017) 623–630.
[54] S. Grimm, The ER–mitochondria interface: the social network of cell death, Biochim. Biophys. Acta, Mol. Cell Res. 1823 (2012) 327–334.
[55] V. Shoshan-Barmatz, D. Mizrachi, VDAC1: from structure to cancer therapy, Front. Oncol. 2 (2012) 1–34.
[56] P. Pinton, C. Giorgi, R. Siviero, E. Zechini, R. Rizzuto, Calcium and apoptosis: ER–mitochondria Ca^{2+} transfer in the control of apoptosis, Oncogene 27 (2008) 6407–6418.
[57] M. Giacomello, I. Drago, P. Pizzo, T. Pozzan, Mitochondrial Ca^{2+} as a key regulator of cell life and death, Cell Death Differ. 14 (2007) 1267–1274.
[58] D. Suen, K.L. Norris, R.J. Youle, Mitochondrial dynamics and apoptosis, Genes Dev. 22 (2008) 1577–1590.
[59] P. Ludovico, F. Sansonetty, M. Côrte-Real, Assessment of mitochondrial membrane potential in yeast cell populations by flow cytometry, Microbiology 147 (2001) 3335–3343.
[60] M. Esposito, S. Piatti, L. Hofmann, L. Frontali, A. Delahodde, T. Rinaldi, Analysis of the rpn11-m1 proteasomal mutant reveals connection between cell cycle and mitochondrial biogenesis, FEMS Yeast Res. 11 (2011) 60–71.
[61] L.F. Sogo, M.P. Yaffe, Regulation of mitochondrial morphology and inheritance by Mdm10p, a protein of the mitochondrial outer membrane, J. Cell Biol. 126 (1994) 1361–1373.
[62] M.J. Youngman, A.E.A. Hobbs, S.M. Burgess, M. Srinivasan, R.E. Jensen, Mmm2p, a mitochondrial outer membrane protein required for yeast mitochondrial shape and maintenance of mtDNA nucleoids, J. Cell Biol. 164 (2004) 677–688.
[63] N. Guaragnella, L. Antonacci, S. Passarella, E. Marra, S. Giannattasio, Achievements and perspectives in yeast acetic acid-induced programmed cell death pathways, Biochem. Soc. Trans. 39 (2011) 1538–1543.
[64] K. Jin, G. Musso, J. Vlasblom, M. Jessulat, V. Deineko, J. Negroni, R. Mosca, R. Malty, D.H. Nguyen-Tran, H. Aoki, Z. Minic, T. Freywald, S. Phanse, Q. Xiang, A. Freywald, P. Aloy, Z. Zhang, M. Babu, Yeast mitochondrial protein–protein interactions reveal diverse complexes and disease-relevant functional relationships, J. Proteome Res. 14 (2015) 1220–1237.
[65] T. Tan, Ö. Cagakan, B. Britta, D. Rapaport, K.S. Dimmer, Mcp1 and Mcp2, two novel proteins involved in mitochondrial lipid homeostasis, J. Cell Sci. 126 (2013) 3563–3574.
[66] M. Ogur, R. St. John, S. Nagai, Tetrazolium overlay technique for population studies of respiration deficiency in yeast, Science 125 (1957) 928–929.
[67] I. Budihardjo, H. Oliver, M. Lutter, X. Luo, X. Wang, Biochemical pathways of caspase activation during apoptosis, Annu. Rev. Cell Dev. Biol. 15 (1999) 269–290.
[68] B. Westermann, Bioenergetic role of mitochondrial fusion and fission, Biochim. Biophys. Acta Bioenerg. 1817 (2012) 1833–1838.
[69] P. Herrero, R. Fernfindez, F. Moreno, Differential sensitivities to glucose and galactose repression of gluconeogenic and respiratory enzymes from *Saccharomyces cerevisiae*, Arch. Microbiol. 143 (1985) 216–219.
[70] X.X. Li, B. Tsoi, Y.F. Li, H. Kurihara, R.R. He, Cardiolipin and its different properties in mitophagy and apoptosis, J. Histochem. Cytochem. 63 (2015) 301–311.
[71] K. Segawa, S. Nagata, An apoptotic "eat me" signal: phosphatidylserine exposure, Trends Cell Biol. 25 (2015) 639–650.
[72] L. Klug, G. Daum, Yeast lipid metabolism at a glance, FEMS Yeast Res. 14 (2014) 369–388.
[73] E. Zinser, C.D.M. Sperka-Gottlieb, E. Fasch, S.D. Kohlwein, F. Paltauf, G. Daum, Phospholipid synthesis and lipid composition of subcellular membranes in the unicellular eukaryote *Saccharomyces cerevisiae*, J. Bacteriol. 173 (1991) 2026–2034.
[74] L. Hedskog, C. Moreira Pinho, R. Filadi, A. Rönnbäck, L. Hertwig, B. Wiehager, P. Larssen, S. Gellhaar, A. Sandebring, M. Westerlund, C. Graff, B. Winblad, D. Galter, H. Behbahani, P. Pizzo, E. Glaser, M. Ankarcrona, Modulation of the endoplasmic reticulum–mitochondria interface in Alzheimer' s disease and related models, Proc. Natl. Acad. Sci. U. S. A. 110 (2013) 7916–7921.
[75] M.S. Herrera-Cruz, T. Simmen, Cancer: untethering mitochondria from the endoplasmic reticulum? Front. Oncol. 7 (2017) 9–13.
[76] S. Marchi, C. Giorgi, M. Oparka, J. Duszynski, M.R. Wieckowski, P. Pinton, Oncogenic and oncosuppressive signal transduction at mitochondria-associated endoplasmic reticulum membranes, Mol. Cell. Oncol. 1 (2014), e956469.
[77] S. Paillusson, R. Stoica, P. Gomez-Suaga, D.H.W. Lau, S. Mueller, T. Miller, C.C.J. Miller, There's something wrong

with my MAM; the ER–mitochondria axis and neurodegenerative diseases, Trends Neurosci. 39 (2016) 146–157.
[78] E. Tubbs, J. Rieusset, Metabolic signaling functions of ER–mitochondria contact sites: role in metabolic diseases, J. Mol. Endocrinol. 58 (2014) R87–106.
[79] E. Zampese, C. Fasolato, M.J. Kipanyula, M. Bortolozzi, T. Pozzan, P. Pizzo, Presenilin 2 modulates endoplasmic reticulum (ER)-mitochondria interactions and Ca^{2+} cross-talk, Proc. Natl. Acad. Sci. 108 (2011) 2777–2782.
[80] N. Guaragnella, A. Bobba, S. Passarella, E. Marra, S. Giannattasio, Yeast acetic acid-induced programmed cell death can occur without cytochrome *c* release which requires metacaspase YCA1, FEBS Lett. 584 (2010) 224–228.
[81] S. Giannattasio, N. Guaragnella, M. Côrte-Real, S. Passarella, E. Marra, Acid stress adaptation protects *Saccharomyces cerevisiae* from acetic acid-induced programmed cell death, Gene 354 (2005) 93–98.
[82] C. Meisinger, M. Rissler, A. Chacinska, L.K. Sanjua, D. Milenkovic, V. Kozjak, C. Lohaus, H.E. Meyer, M.P. Yaffe, B. Guiard, N. Wiedemann, N. Pfanner, The mitochondrial morphology protein Mdm10 functions in assembly of the preprotein translocase of the outer membrane, Dev. Cell 7 (2004) 61–71.
[83] K. Yamano, S. Tanaka-Yamano, T. Endo, Tom7 regulates Mdm10-mediated assembly of the mitochondrial import channel protein TOM40, J. Biol. Chem. 285 (2010) 41222–41231.
[84] M. Ott, E. Norberg, K.M. Walter, P. Schreiner, C. Kemper, D. Rapaport, B. Zhivotovsky, S. Orrenius, The mitochondrial TOM complex is required for tBid/Bax-induced cytochrome *c* release, J. Biol. Chem. 282 (2007) 27633–27639.
[85] L.K. Sanjuán Szklarz, V. Kozjak-Pavlovic, F.N. Vögtle, A. Chacinska, D. Milenkovic, S. Vogel, M. Dürr, B. Westermann, B. Guiard, J.C. Martinou, C. Borner, N. Pfanner, C. Meisinger, Preprotein transport machineries of yeast mitochondrial outer membrane are not required for Bax-induced release of intermembrane space proteins, J. Mol. Biol. 368 (2007) 44–54.
[86] D. De Stefani, A. Raffaello, E. Teardo, I. Szabò, R. Rizzuto, A 40 kDa protein of the inner membrane is the mitochondrial calcium uniporter, Nature 476 (2011) 336–340.
[87] F. Madeo, E. Fröhlich, K.U. Fröhlich, A yeast mutant showing diagnostic markers of early and late apoptosis, J. Cell Biol. 139 (1997) 729–734.
[88] C. Osman, M. Haag, C. Potting, J. Rodenfels, P.V. Dip, F.T. Wieland, B. Brügger, B. Westermann, T. Langer, The genetic interactome of prohibitins: coordinated control of cardiolipin and phosphatidylethanolamine by conserved regulators in mitochondria, J. Cell Biol. 184 (2009) 583–596.
[89] M. Sinzel, T. Tan, P. Wendling, H. Kalbacher, C. Özbalci, X. Chelius, B. Westermann, B. Brügger, D. Rapaport, K.S. Dimmer, Mcp 3 is a novel mitochondrial outer membrane protein that follows a unique IMP-dependent biogenesis pathway, EMBO Rep. 17 (2016) 965–981.
[90] Y. Tamura, O. Onguka, A.E. Aiken Hobbs, R.E. Jensen, M. Iijima, S.M. Claypool, H. Sesaki, Role for two conserved intermembrane space proteins, Ups1p and Up2p, in intramitochondrial phospholipid trafficking, J. Biol. Chem. 287 (2012) 15205–15218.
[91] K. Yamano, S. Tanaka-Yamano, T. Endo, Mdm10 as a dynamic constituent of the TOB/SAM complex directs coordinated assembly of Tom40, EMBO Rep. 11 (2010) 187–193.
[92] C. Voss, S. Lahiri, B.P. Young, C.J. Loewen, W.A. Prinz, ER-shaping proteins facilitate lipid exchange between the ER and mitochondria in *S. cerevisiae*, J. Cell Sci. 125 (2012) 4791–4799.
[93] S. Lahiri, J.T. Chao, S. Tavassoli, A.K.O. Wong, V. Choudhary, B.P. Young, C.J.R. Loewen, W.A. Prinz, A conserved endoplasmic reticulum membrane protein complex (EMC) facilitates phospholipid transfer from the ER to mitochondria, PLoS Biol. 12 (2014).
[94] M. Kannan, C. Sivaprakasam, W.A. Prinz, V. Nachiappan, Endoplasmic reticulum stress affects the transport of phosphatidylethanolamine from mitochondria to the endoplasmic reticulum in *S. cerevisiae*, Biochim. Biophys. Acta Mol. Cell Biol. Lipids 1861 ((2016) 1959–1967.
[95] H. Jeong, J. Park, C. Lee, Crystal structure of Mdm12 reveals the architecture and dynamic organization of the ERMES complex, EMBO Rep. 17 (2016) 1857–1871.
[96] T.K. Rostovtseva, S.M. Bezrukov, VDAC regulation: role of cytosolic proteins and mitochondrial lipids, J. Bioenerg. Biomembr. 40 (2008) 163–170.
[97] J.R. Friedman, M. Kannan, A. Toulmay, C.H. Jan, J.S. Weissman, W.A. Prinz, J. Nunnari, Lipid homeostasis is maintained by dual targeting of the mitochondrial PE biosynthesis enzyme to the ER, Dev. Cell 44 (2018) 1–10.
[98] P. Rockenfeller, M. Koska, F. Pietrocola, N. Minois, O. Knittelfelder, V. Sica, J. Franz, G. Kroemer, F. Madeo, Phosphatidylethanolamine positively regulates autophagy and longevity, Cell Death Differ. 22 (2015) 499–508.
[99] E. Rosivatz, R. Woscholski, Removal or masking of phosphatidylinositol(4,5)bisphosphate from the outer mitochondrial membrane causes mitochondrial fragmentation, Cell. Signal. 23 (2011) 478–486.
[100] N. Kawazoe, Y. Kimata, S. Izawa, Acetic acid causes endoplasmic reticulum stress and induces the unfolded protein response in *Saccharomyces cerevisiae*, Front. Microbiol. 8 (2017) 1–10.
[101] R. Sano, J.C. Reed, ER stress-induced cell death mechanisms, Biochim. Biophys. Acta, Mol. Cell Res. 1833 (2013) 3460–3470.
[102] C.B. Brachmann, A. Davies, G.J. Cost, E. Caputo, J. Li, P. Hieter, J.D. Boeke, Designer deletion strains derived from *Saccharomyces cerevisiae* S288C: a useful set of strains and plasmids for PCR-mediated gene disruption and other applications, Yeast 14 (1998) 115–132.
[103] R.D. Gietz, R.A. Woods, Yeast transformation by the LiAc/SS carrier DNA/PEG method, Methods Mol. Biol. 313 (2006) 107–120.
[104] C. Meisinger, N. Pfanner, K.N. Truscott, Isolation of yeast mitochondria, Yeast Protoc 2006, pp. 33–39.
[105] M.M. Bradford, A rapid and sensitive method for the quantitation of microgram quantities of protein utilizing the principle of protein-dye binding, Anal. Biochem. 72 (1976) 248–254.
[106] E.G. Bligh, W.J. Dyer, A rapid method of total lipid extraction and purification, Can. J. Biochem. Physiol. 37 (1959) 911–917.
[107] D.R. Santinha, M. Luísa Dória, B.M. Neves, E.A. Maciel, J. Martins, L. Helguero, P. Domingues, M. Teresa Cruz, M. Rosário Domingues, Prospective phospholipid markers for skin sensitization prediction in keratinocytes: a phospholipidomic approach, Arch. Biochem. Biophys. 533 (2013) 33–41.
[108] E.M. Bartlett, D.H. Lewis, Spectrophotometric determination of phosphate esters in the presence and absence of orthophosphate, Anal. Biochem. 36 (1970) 159–167.
[109] G. Rouser, S. Fleischer, A. Yamamoto, Two dimensional thin layer chromatographic separation of polar lipids and determination of phospholipids by phosphorus analysis of spots, Lipids 5 (1970) 494–496.